

Interpreting the 750 GeV diphoton signal as technipion

Piotr LEBIEDOWICZ

Institute of Nuclear Physics, Polish Academy of Sciences, PL-31-342 Cracow, Poland

E-mail: Piotr.Lebiedowicz@ifj.edu.pl

Marta ŁUSZCZAK

Department of Theoretical Physics, University of Rzeszów, PL-35-959 Rzeszów, Poland

E-mail: luszczak@univ.rzeszow.pl

Roman PASECHNIK

Department of Astronomy and Theoretical Physics, Lund University, SE-223 62 Lund, Sweden

E-mail: Roman.Pasechnik@thep.lu.se

Antoni SZCZUREK*

Institute of Nuclear Physics, Polish Academy of Sciences, PL-31-342 Cracow, Poland[†]

E-mail: Antoni.Szczurek@ifj.edu.pl

We discuss whether the enhancement in the diphoton final state at $M_{\gamma\gamma} = 750$ GeV, observed recently by the ATLAS and CMS Collaborations could be a neutral pseudoscalar technipion $\tilde{\pi}^0$. We considered two distinct minimal models for the dynamical electroweak symmetry breaking. Here we concentrate only on two-flavor vector-like technicolor model and we assume that the two-photon fusion is a dominant production mechanism. We include contributions of $2 \rightarrow 1$, $2 \rightarrow 2$ and $2 \rightarrow 3$ partonic processes. All the mechanisms give similar contributions to the cross section. With the strong Yukawa (technipion-techniquark) coupling $g_{TC} \simeq 20$ we roughly obtain the measured cross section of the “signal”. With such value of g_{TC} we get a relatively small total decay width Γ_{tot} . We discuss also the size of the signal at lower energies (LHC, Tevatron) for $\gamma\gamma$ final states, where the enhancement was not observed. We predict a measurable cross section for neutral technipion production associated with one or two soft jets. The technipion signal is compared with the Standard Model diphoton background contributions. We observe the dominance of inelastic-inelastic $\gamma\gamma$ processes. We predict the signal cross section for purely exclusive $pp \rightarrow pp\gamma\gamma$ processes at $\sqrt{s} = 13$ TeV to be about 0.2 fb. Such a cross section would be, however, difficult to measure with the planned integrated luminosity. We conclude that in all considered cases the signal is below the background or/and below the threshold set by statistics although some tension can be seen.

XXIV International Workshop on Deep-Inelastic Scattering and Related Subjects

11-15 April, 2016

DESY Hamburg, Germany

*Speaker.

[†]Also at University of Rzeszów, PL-35-959 Rzeszów, Poland.

1. Introduction

Recently both the ATLAS and CMS Collaborations announced an observation of an enhancement in the diphoton invariant mass at $M_{\gamma\gamma} \approx 750$ GeV in proton-proton collisions at $\sqrt{s} = 13$ TeV [1, 2, 3, 4]. Remarkably, such a hint to a possible New Physics signal has triggered a lot of activities recently. Several possible interpretations were discussed (see for instance [5]).

One of the appealing and consistent classes of technicolor (TC) models with a vector-like (Dirac) UV completion is known as the vector-like TC (VTC) scenario [6]. The simplest version of the VTC scenario applied to the EWSB possessed two Dirac techniflavors and a SM-like Higgs boson [7, 8, 9]. Recently, the concept of Dirac UV completion has also emerged in composite Higgs boson scenarios with confined $SU(2)_{TC}$ symmetry [10, 11].

The mechanisms considered in our recent paper [12] are shown in Figs. 1-3.

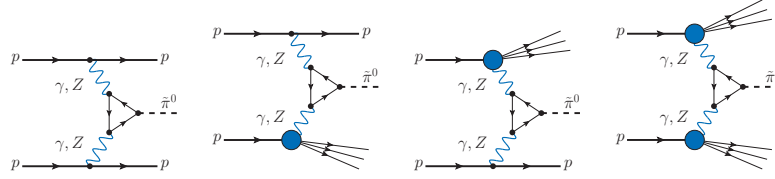


Figure 1: Diagrams of neutral technipion production via the $\gamma\gamma$, γZ and ZZ fusion in pp -collisions.

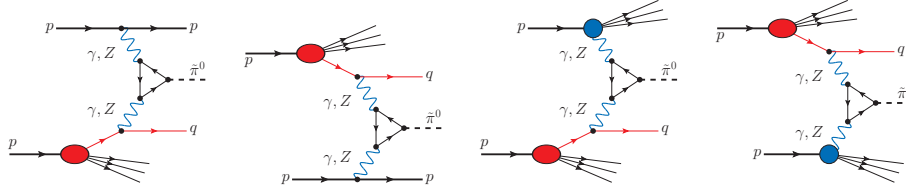


Figure 2: Technipion production via the $2 \rightarrow 2$ partonic subprocesses.

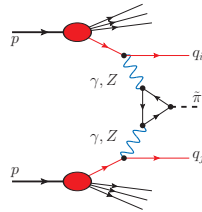


Figure 3: Technipion production via the $2 \rightarrow 3$ partonic subprocesses.

2. An example of the amplitude calculation

In the case of VTC technipion model [7], the amplitude for the $\gamma\gamma \rightarrow \tilde{\pi}^0 \rightarrow \gamma\gamma$ subprocess reads:

$$\begin{aligned} \mathcal{M}_{\gamma\gamma \rightarrow \tilde{\pi}^0 \rightarrow \gamma\gamma}(\lambda_1, \lambda_2, \lambda_3, \lambda_4) &= (\epsilon^{(\gamma)\mu_3}(p_3, \lambda_3))^* (\epsilon^{(\gamma)\mu_4}(p_4, \lambda_4))^* \\ &\times \epsilon_{\mu_3\mu_4\nu_3\nu_4} p_3^{\nu_3} p_4^{\nu_4} F_{\gamma\gamma} \frac{i}{\hat{s} - m_{\tilde{\pi}^0}^2 + im_{\tilde{\pi}^0}\Gamma_{tot}} \epsilon_{\mu_1\mu_2\nu_1\nu_2} p_1^{\nu_1} p_2^{\nu_2} F_{\gamma\gamma} \epsilon^{(\gamma)\mu_1}(p_1, \lambda_1) \epsilon^{(\gamma)\mu_2}(p_2, \lambda_2), \end{aligned} \quad (2.1)$$

Table 1: Hadronic cross section in fb for technipion production for different contributions, see Figs. 1-3.

Component	$\sqrt{s} = 1.96 \text{ TeV}$	7 TeV	8 TeV	13 TeV	100 TeV
$2 \rightarrow 1 \text{ (in, in)}$	1.37×10^{-3}	0.16	0.22	0.55	8.08
$2 \rightarrow 1 \text{ (in, el)}$	0.22×10^{-3}	0.05	0.06	0.15	1.88
$2 \rightarrow 1 \text{ (el, in)}$	0.22×10^{-3}	0.05	0.06	0.15	1.88
$2 \rightarrow 1 \text{ (el, el)}$	0.03×10^{-3}	0.01	0.02	0.04	0.42
$2 \rightarrow 1, \text{ sum of all}$	1.84×10^{-3}	0.27	0.36	0.89	12.26
$2 \rightarrow 2 \text{ (in, in), two diagrams}$	0.74×10^{-3}	0.14	0.19	0.49	7.69
$2 \rightarrow 2 \text{ (in, el) and (el, in)}$	0.13×10^{-3}	0.05	0.07	0.19	2.93
$2 \rightarrow 2, \text{ sum of all}$	0.87×10^{-3}	0.19	0.26	0.68	10.62
$2 \rightarrow 2, \text{ sum of all, } p_{t,jet} > 10 \text{ GeV}$				0.43	8.03
$2 \rightarrow 2, \text{ sum of all, } p_{t,jet} > 20 \text{ GeV}$				0.35	6.99
$2 \rightarrow 2, \text{ sum of all, } p_{t,jet} > 50 \text{ GeV}$				0.25	5.42
$2 \rightarrow 3$	0.14×10^{-3}	0.09	0.13	0.46	16.71
$2 \rightarrow 3, p_{t,jet} > 10 \text{ GeV}$				0.04	1.41

where the effective neutral technipion coupling $F_{\gamma\gamma}$ is [7]

$$F_{\gamma\gamma} = \frac{4\alpha_{em} g_{TC}}{\pi} \frac{m_{\tilde{Q}}}{m_{\tilde{\pi}^0}^2} \arcsin^2\left(\frac{m_{\tilde{\pi}^0}}{2m_{\tilde{Q}}}\right), \quad \frac{m_{\tilde{\pi}^0}}{2m_{\tilde{Q}}} < 1. \quad (2.2)$$

The Γ_{tot} can be calculated from a model or taken from recent experimental data. In the following we take the calculated value of Γ_{tot} and $m_{\tilde{\pi}^0} = 750 \text{ GeV}$. The mass scale of the degenerate techniquarks $m_{\tilde{Q}}$ is in principle another free parameter (see Ref. [8]).

The cross section for the signal is calculated as ($\mu_F^2 = p_{t,\gamma}^2$):

$$\frac{d\sigma}{dy_3 dy_4 d^2 p_{t,\gamma}} = \frac{1}{16\pi^2 \hat{s}^2} \sum_{ij} x_1 \gamma^{(i)}(x_1, \mu_F^2) x_2 \gamma^{(j)}(x_2, \mu_F^2) |\overline{\mathcal{M}}_{\gamma\gamma \rightarrow \tilde{\pi}^0 \rightarrow \gamma\gamma}|^2, \quad (2.3)$$

where $i, j = \text{el or in}$, i.e. they correspond to elastic or inelastic fluxes (x -distributions) of equivalent photons, respectively, and x_1, x_2 are the longitudinal momentum fractions of the proton

$$x_1 = \frac{p_{t,\gamma}}{\sqrt{s}} [\exp(y_3) + \exp(y_4)], \quad x_2 = \frac{p_{t,\gamma}}{\sqrt{s}} [\exp(-y_3) + \exp(-y_4)]. \quad (2.4)$$

3. Selected results

We summarize our results in Table 1 where we have collected cross sections for different QED orders shown in the figures above. The elastic photon fluxes were calculated using the Drees-Zeppenfeld parametrization [13, 14], where a simple parametrization of the nucleon electromagnetic form factors is used. To calculate inelastic contributions we use collinear approach with photon MRST(QED) parton distributions [15]. Surprisingly, different contributions are of the same order of magnitude. In this calculation $g_{TC} = 10$ and $m_{\tilde{Q}} = 0.75 m_{\tilde{\pi}^0}$ were used. To describe the experimental signal more precisely g_{TC} can be rescaled.

The dependence of the cross section on g_{TC} is shown in Fig 4 for $\sqrt{s} = 8 \text{ TeV}$ (left panel) and $\sqrt{s} = 13 \text{ TeV}$ (right panel) within an experimental uncertainties taken from [5] (narrow width scenario). Our result for $g_{TC} = 20$ and our standard choice $m_{\tilde{Q}} = 0.75 m_{\tilde{\pi}^0}$ is at the lower edge of

experimental uncertainties at $\sqrt{s} = 13$ TeV and at the upper edge of experimental uncertainties at $\sqrt{s} = 8$ TeV. If $m_{\tilde{Q}}/m_{\tilde{\pi}}^0$ is smaller the g_{TC} could be lower, see Fig. 8 of [8]. The value of $g_{TC} = 20$ could be smaller when exchange of Z bosons is included.

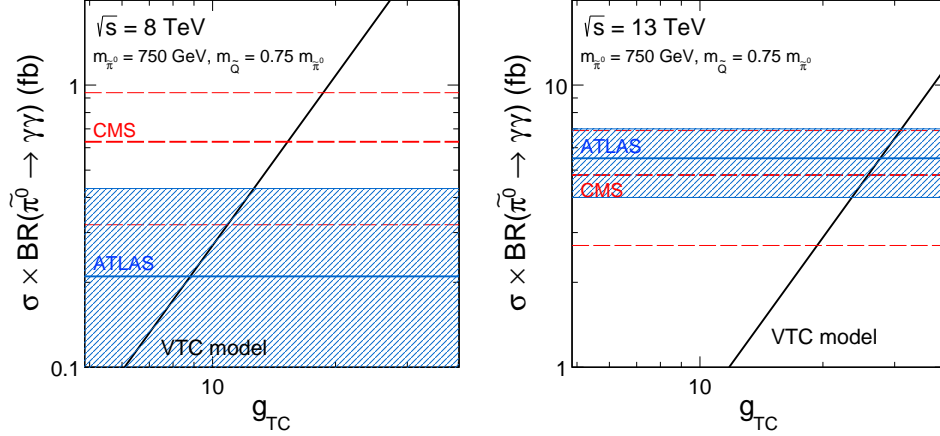


Figure 4: The dependence of the hadronic $pp \rightarrow (\tilde{\pi}^0 \rightarrow \gamma\gamma) + X$ cross section on g_{TC} together with the crudely estimated in [5] experimental result at the LHC [3, 4]. The solid black line represents our result for the technipion production in the VTC model.

The most important is the distribution in diphoton invariant mass where the signal was observed. In Fig. 5 we show four examples relevant for different experiments using their kinematic conditions: D0 at $\sqrt{s} = 1.96$ TeV [17], ATLAS at $\sqrt{s} = 7$ TeV [18], ATLAS at $\sqrt{s} = 13$ TeV [3], and the prediction for Future Circular Collider at $\sqrt{s} = 100$ TeV. We show both signal and background contributions. Clearly the $q\bar{q}$ annihilation contribution dominates, especially at large invariant masses in the surrounding of the signal. In our analysis the experimental invariant mass resolution was included for the signal-technipion calculations in the following simple way

$$\frac{d\sigma}{dM_{\gamma\gamma}} = \sigma_{\tilde{\pi}^0} \frac{1}{\sqrt{2\pi}\sigma} \exp\left(-\frac{(M_{\gamma\gamma} - m_{\tilde{\pi}^0})^2}{2\sigma^2}\right). \quad (3.1)$$

In the calculation we take $\sigma = 15$ GeV assuming $\sigma/m_{\tilde{\pi}^0} \sim 2\%$. In Eq. (3.1) we take $\sigma_{\tilde{\pi}^0} = 0.005$ fb, 1.09 fb, 2.36 fb, 24.83 fb corresponding to $\sqrt{s} = 1.96, 7, 13, 100$ TeV, respectively, including the relevant kinematical cuts shown in the panels of Fig. 5. The values of cross sections above were obtained from Eq. (2.3) and $g_{TC} = 20$.

4. Conclusions

In our recent paper [12] we discussed a possibility that recently observed by the ATLAS and CMS Collaborations diphoton enhancement at invariant mass $M_{\gamma\gamma} \approx 750$ GeV is a technipion. The main emphasis was put on chirally-symmetric (vector-like) Technicolor model with two mass degenerate (techni)flavours. In this model only $\gamma\gamma$, γZ and ZZ couplings and production mechanisms are possible. Therefore the decay width is rather small $\Gamma_{tot} \ll 1$ GeV.

We discussed there in detail the production mechanisms within the considered model. In the present version we included only photon initiated processes. In some modern parton distribution

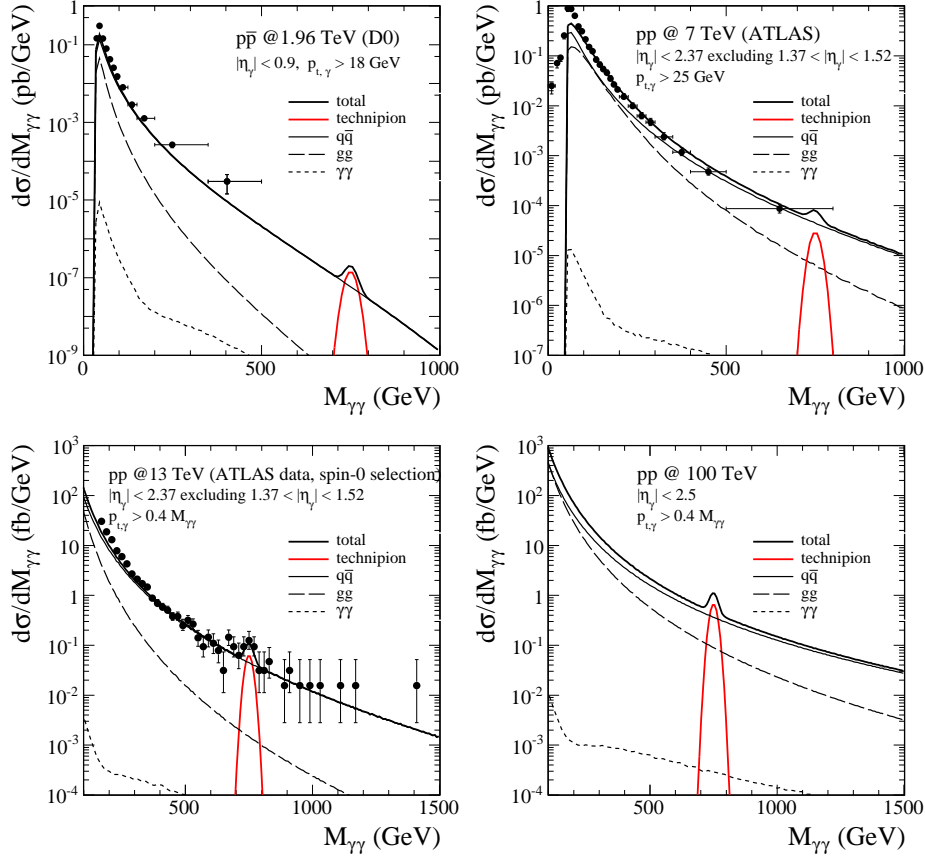


Figure 5: The two-photon invariant mass distributions for different background contributions and the signal-technipion predictions obtained in the VTC model including experimental cuts. For comparison, the experimental data from D0 [17] at $\sqrt{s} = 1.96$ TeV, ATLAS at $\sqrt{s} = 7$ TeV [18], the recent ATLAS data (spin-0 selection) at $\sqrt{s} = 13$ TeV [3] and our prediction for Future Circular Collider are presented.

models photons are included as partons in the proton. In this model there is a reach pattern of electroweak contributions. We have considered $2 \rightarrow 1$, $2 \rightarrow 2$ and $2 \rightarrow 3$ type processes. We have found that they give similar contributions to the cross section. In order to describe the observed “signal” we had to adjust model coupling of techniquarks to the neutral technipion. Including the photon initiated processes only we have found that $g_{TC} \simeq 20$ is not inconsistent with the experimental data.

In addition, we have made predictions for the Tevatron, Run-I LHC and Future Circular Collider. The predictions for the Tevatron have been discussed in the context of existing data in the diphoton channel. We have concluded that the cross section for energies lower than 8 TeV are so small (below background for integrated luminosity limit) that the signal could not be observed.

We have also made predictions for purely exclusive case. We have predicted the cross section of the order of 0.2 fb at $\sqrt{s} = 13$ TeV. To focus on such a case one has to measure technipion (two photons) in the central detectors as well as both protons in forward directions.

In Ref. [12] we considered also an alternative one-family walking technicolor model discussed recently in Ref. [16] (see also references therein). In this model the gluon-gluon fusion is the dominant production mechanism of assumed isoscalar technipion. We refer to [12] for details of

the corresponding analysis.

In summary, the considered technicolor models cannot be excluded by the present $\gamma\gamma$ and dijet data [19, 20].

This research was partially supported by the Polish National Science Centre Grants DEC-2013/09/D/ST2/03724 and DEC-2014/15/B/ST2/02528 and by the Centre for Innovation and Transfer of Natural Sciences and Engineering Knowledge in Rzeszów. R. P. was partially supported by the Swedish Research Council Grant No. 2013-4287.

References

- [1] (ATLAS Collaboration), ATLAS-CONF-2015-081 (2015).
- [2] V. Khachatryan *et al.*, (CMS Collaboration), CMS PAS EXO-15-004 (2015).
- [3] M. Aaboud *et al.*, (ATLAS Collaboration), CERN-EP-2016-120, arXiv:1606.03833 [hep-ex].
- [4] V. Khachatryan *et al.*, (CMS Collaboration), CMS-EXO-16-018, CERN-EP-2016-154, arXiv:1606.04093 [hep-ex].
- [5] A. Strumia, arXiv:1605.09401 [hep-ph].
- [6] C. Kilic, T. Okui, and R. Sundrum, JHEP **02** (2010) 018, arXiv:0906.0577 [hep-ph].
- [7] R. Pasechnik, V. Beylin, V. Kuksa, and G. Vereshkov, Phys. Rev. **D88** (2013) 075009, arXiv:1304.2081 [hep-ph].
- [8] P. Lebiedowicz, R. Pasechnik, and A. Szczurek, Nucl. Phys. **B881** (2014) 288, arXiv:1309.7300 [hep-ph].
- [9] R. Pasechnik, V. Beylin, V. Kuksa, and G. Vereshkov, Int. J. Mod. Phys. **A31** (2016) 1650036, arXiv:1407.2392 [hep-ph].
- [10] G. Cacciapaglia and F. Sannino, JHEP **04** (2014) 111, arXiv:1402.0233 [hep-ph].
- [11] A. Hietanen, R. Lewis, C. Pica, and F. Sannino, JHEP **07** (2014) 116, arXiv:1404.2794 [hep-lat].
- [12] P. Lebiedowicz, M. Łuszczak, R. Pasechnik, and A. Szczurek, arXiv:1604.02037 [hep-ph].
- [13] M. Drees and D. Zeppenfeld, Phys. Rev. **D39** (1989) 2536.
- [14] M. Drees, R. M. Godbole, M. Nowakowski, and S. D. Rindani, Phys. Rev. **D50** (1994) 2335.
- [15] A. D. Martin, R. G. Roberts, W. J. Stirling, and R. S. Thorne, Eur. Phys. J. **C39** (2005) 155.
- [16] S. Matsuzaki and K. Yamawaki, arXiv:1512.05564 [hep-ph].
- [17] V. M. Abazov *et al.*, (D0 Collaboration), Phys. Lett. **B725** (2013) 6.
- [18] G. Aad *et al.*, (ATLAS Collaboration), JHEP **01** (2013) 086, arXiv:1211.1913 [hep-ex].
- [19] T. Aaltonen *et al.*, (CDF Collaboration), Phys. Rev. **D79** (2009) 112002, arXiv:0812.4036 [hep-ex].
- [20] G. Aad *et al.*, (ATLAS Collaboration), JHEP **05** (2014) 059, arXiv:1312.3524 [hep-ex].